Dielectric polarization and refractive indices of ultrathin barium titanate films on strontium titanate single crystals

2005 J. Phys.: Condens. Matter 17 161

(http://iopscience.iop.org/0953-8984/17/1/015)

INSTITUTE OF PHYSICS PUBLISHING JOURNAL OF PHYSICS: CONDENSED MATTER

J. Phys.: Condens. Matter **17** (2005) 161–179 doi:10.1088/0953-8984/17/1/015

Dielectric polarization and refractive indices of ultrathin barium titanate films on strontium titanate single crystals

H Chaib, L M Eng and T Otto

Institute of Applied Photophysics, University of Technology Dresden, D-01062 Dresden, Germany

E-mail: eng@iapp.de

Received 25 October 2004, in final form 23 November 2004
Published 10 December 2004
Online at stacks.iop.org/JPhysCM/17/161

Abstract

The electrical and optical properties of ultrathin films of tetragonal barium titanate ($BaTiO_3$) on strontium titanate ($SrTiO_3$) single-crystal substrates are theoretically investigated using a microscopic quantum mechanical model based on the orbital approximation in correlation with the dipole–dipole interaction. First-, second-, and third-order electronic polarizabilities had to be considered in this calculation in order to obtain accurate results for both the dielectric spontaneous polarization and the refractive indices of the $BaTiO_3$ overlayer. The spontaneous polarization is drastically reduced in the film as its thickness decreases. However, an electronic polarization appears within the $SrTiO_3$ substrate in the neighbourhood of the interface. This polarization, which vanishes far away from the interface into the $SrTiO_3$ bulk, is induced by the polarization of the $BaTiO_3$ film. Furthermore, we find the refractive index for both the $BaTiO_3$ film and the $SrTiO_3$ substrate to be deeply reduced for light polarized perpendicular to the surface.

(Some figures in this article are in colour only in the electronic version)

1. Introduction

Tetragonal barium titanate ($BaTiO_3$) is a ferroelectric oxide material of great importance for potential applications due to its unusual piezoelectric, ferroelectric, dielectric, optical, electro-optic, and photorefractive properties. Many of these applications are increasingly oriented towards thin films [1–11] and superlattice geometries [12–16], where interfaces and/or surface properties are of importance. Strontium titanate ($SrTiO_3$) is one of the materials of choice for growing $BaTiO_3$ thin films, and also for stacked superlattices ($BaTiO_3/SrTiO_3$) due to their relatively low atomic misfit. At room temperature, $SrTiO_3$ is a centrosymmetric paraelectric material with a cubic structure having a lattice parameter ($a = 3.905$ Å) [5] close to that

of tetragonal $BaTiO_3$ ($a = 3.992$ Å) [17] with a difference of about $\sim$2%. This mismatch between the in-plane lattice parameters of $BaTiO_3$ and $SrTiO_3$ is the cause of the lattice strain induced in the thin $BaTiO_3$ films as well as for periodically stacked layers in the superlattice structures.

Here we present a quantum mechanical theoretical approach for studying the spontaneous polarization and refractive indices of $BaTiO_3$ thin films grown on $SrTiO_3$ substrates at room temperature. Our microscopic model takes into account the anisotropy in the first-, second-, and third-order electronic polarizabilities of all constituent ions, their ionic shifts, as well as the crystalline deformations. The model was previously tested for the calculation of bulk properties of mono-domain tetragonal perovskites such as tetragonal $BaTiO_3$ and $KNbO_3$, i.e. their ferroelectricity and optical anisotropy as well as their linear electro-optical coefficients [18]. Furthermore, the same model was successfully applied for modelling electrical and optical properties of rhombohedral $LiNbO_3$ single crystals [19], as well as 90° and 180° ferroelectric domain walls in $BaTiO_3$.

On the basis of those experiences which agree excellently with the corresponding experimental data, we initiate here the application of this model to $BaTiO_3$ thin films in the tetragonal phase. The model accounts for the following points:

- expansion of the local electric field, by simultaneously considering the field components $\mathbf{E}_k^{\mathrm{loc}}$ in all directions;
- representation of the local electric field in a tensorial equation, allowing one to describe all $\mathbf{E}_k^{\mathrm{loc}}$ for all ions simultaneously;
- development of the orbital approximation, by taking into account the anisotropy in the first-, second-, and third-order electronic polarizabilities of the constituent ions;
- consideration of the correlation between the first-, second-, and third-order electronic polarizabilities on one hand, and their dependence on the local electric field on the other hand;
- calculating the surface and interface effects resulting in a reduced spherical Lorentz cavity.

The paper is structured as follows. Section 2 briefly discusses the first-, second-, and third-order electronic polarizabilities of the constituent ions in both tetragonal $BaTiO_3$ (film) and cubic $SrTiO_3$ (substrate) by using the quantum mechanical method based on the orbital approximation. Next we discuss the dipole–dipole interaction due to the local electric field acting on the constituent ions taking into account the crystalline deformations and individual ionic shifts near the film surface and at the film/substrate interface. Section 3 then presents the results obtained for the spontaneous polarization as well as the refractive indices calculated for the $BaTiO_3$ on $SrTiO_3$ system at room temperature. This section also contains a discussion of the above-mentioned findings.

2. Description of the model

2.1. Orbital approximation

In order to compute the first-, second-, and third-order electronic polarizabilities of the constituent ions of both $BaTiO_3$ (film) and $SrTiO_3$ (substrate), we use a quantum mechanical approach based upon the orbital approximation. This approach describes each ion/atom as a core consisting of all inner electrons and the nucleus, and a shell that carries the outer electron. The electronic dipole moment $\mathbf{p}_l^{\mathrm{e}}$ along the l-direction of this core–shell system may

be expressed as [19]

$$p_l^{\mathrm{e}} \cong \frac{4\langle x_3^2\rangle\langle x_l^2\rangle}{a_B}\left[1 - \frac{8\,\langle x_3^2\rangle^3}{a_B^2 e^2}E^2 + \frac{96\,\langle x_3^2\rangle^6}{a_B^4 e^4}E^4 - \frac{576\,\langle x_3^2\rangle^9}{a_B^6 e^6}E^6\right]E_l. \tag{1}$$

The (k,l) element of the first-order electronic polarizability tensor, the (k,l,l') element of the second-order electronic polarizability tensor (also called the first-order electronic hyperpolarizability), and the (k,l,l',l'') element of the third-order electronic polarizability tensor (also called the second-order electronic hyperpolarizability) are determined, respectively, as follows [20]:

$$\alpha_{kl} = \frac{\partial p_k}{\partial E_l}, \tag{2}$$

$$\beta_{kll'} = \frac{\partial^2 p_k}{\partial E_l\,\partial E_{l'}}, \tag{3}$$

$$\gamma_{kll'l''} = \frac{\partial^3 p_k}{\partial E_l\,\partial E_{l'}\,\partial E_{l''}}. \tag{4}$$

Following equation (1), α_{kl}, $\beta_{kll'}$, and $\gamma_{kll'l''}$ are described for any orbital r as

$$\alpha_{kl,r} = \alpha^*_{k,r}[\delta_{kl} - \theta^*_r(E^2\delta_{kl} + 2\,E_kE_l) + \xi^*_r(E^4\delta_{kl} + 4\,E^2E_kE_l) - \zeta^*_r(E^6\delta_{kl} + 6\,E^4E_kE_l)], \tag{5}$$

$$\begin{aligned}\beta_{kll',r} = \alpha^*_{k,r}[&-2\theta^*_r(E_{l'}\delta_{kl} + E_k\delta_{ll'} + E_l\delta_{kl'})\\ &+ 4\xi^*_r(E^2E_{l'}\delta_{kl} + E^2E_k\delta_{ll'} + E^2E_l\delta_{kl'} + 2E_kE_lE_{l'})\\ &- 6\zeta^*_r(E^4E_{l'}\delta_{kl} + E^4E_k\delta_{ll'} + E^4E_l\delta_{kl'} + 4E^2E_kE_lE_{l'})],\end{aligned} \tag{6}$$

$$\begin{aligned}\gamma_{kll'l'',r} = \alpha^*_{k,r}[&-2\theta^*_r(\delta_{kl}\delta_{l'l''} + \delta_{kl'}\delta_{ll''} + \delta_{kl''}\delta_{ll'}) + 4\xi^*_r(2E_kE_l\delta_{l'l''} + 2E_kE_{l'}\delta_{ll''} + 2E_kE_{l''}\delta_{ll'}\\ &+ 2E_lE_{l'}\delta_{kl''} + 2E_lE_{l''}\delta_{kl'} + 2E_{l'}E_{l''}\delta_{kl} + E^2\delta_{kl}\delta_{l'l''} + E^2\delta_{kl'}\delta_{ll''} + E^2\delta_{kl''}\delta_{ll'})\\ &- 6\zeta^*_r(4E^2E_kE_l\delta_{l'l''} + 4E^2E_kE_{l'}\delta_{ll''} + 4E^2E_kE_{l''}\delta_{ll'}\\ &+ 4E^2E_lE_{l'}\delta_{kl''} + 4E^2E_lE_{l''}\delta_{kl'} + 4E^2E_{l'}E_{l''}\delta_{kl}\\ &+ E^4\delta_{kl}\delta_{l'l''} + E^4\delta_{kl'}\delta_{ll''} + E^4\delta_{kl''}\delta_{ll'} + 8E_kE_lE_{l'}E_{l''})],\end{aligned} \tag{7}$$

where

$$\alpha^*_{k,r} = \frac{4\langle x_3^2\rangle_r\langle x_k^2\rangle_r}{a_B}, \tag{8}$$

$$\theta^*_r = \frac{8\,\langle x_3^2\rangle_r^3}{a_B^2e^2}, \tag{9}$$

$$\xi^*_r = \frac{96\,\langle x_3^2\rangle_r^6}{a_B^4e^4}, \tag{10}$$

$$\zeta^*_r = \frac{576\,\langle x_3^2\rangle_r^9}{a_B^6e^6}. \tag{11}$$

In equations (5)–(7), δ_{kl} represents the Kronecker symbol. We assume the first-, second-, and third-order electronic polarizabilities of a j-ion being considered to result from summing over all contributions of respective orbitals, namely

$$\alpha_{kl}(j) = \sum_r \alpha_{kl,r}(j), \tag{12}$$

$$\beta_{kll'}(j) = \sum_r \beta_{kll',r}(j), \tag{13}$$

$$\gamma_{kll'l''}(j) = \sum_r \gamma_{kll'l'',r}(j). \tag{14}$$

Equations (12)–(14) can be rearranged into

$$\begin{aligned}\alpha_{kl}(j) = \alpha_k^*(j)\{&\delta_{kl} - \theta_k(j)[E^2(j)\delta_{kl} + 2\,E_k(j)E_l(j)] \\ &+ \xi_k(j)[E^4(j)\delta_{kl} + 4\,E^2(j)E_k(j)E_l(j)] \\ &- \zeta_k(j)[E^6(j)\delta_{kl} + 6\,E^4(j)E_k(j)E_l(j)]\}, \end{aligned} \tag{15}$$

$$\begin{aligned}\beta_{kll'}(j) = \alpha_k^*(j)\{&-2\theta_k(j)[E_{l'}(j)\delta_{kl} + E_k(j)\delta_{ll'} + E_l(j)\delta_{kl'}] \\ &+ 4\xi_k(j)[E^2(j)E_{l'}(j)\delta_{kl} + E^2(j)E_k(j)\delta_{ll'} \\ &+ E^2(j)E_l(j)\delta_{kl'} + 2E_k(j)E_l(j)E_{l'}(j)] \\ &- 6\zeta_k(j)[E^4(j)E_{l'}(j)\delta_{kl} + E^4(j)E_k(j)\delta_{ll'} \\ &+ E^4(j)E_l(j)\delta_{kl'} + 4E^2(j)E_k(j)E_l(j)E_{l'}(j)]\}, \end{aligned} \tag{16}$$

$$\begin{aligned}\gamma_{kll'l''}(j) = \alpha_k^*(j)\{&-2\theta_k(j)[\delta_{kl}\delta_{l'l''} + \delta_{kl'}\delta_{ll''} + \delta_{kl''}\delta_{ll'}] \\ &+ 4\xi_k(j)[2E_k(j)E_l(j)\delta_{l'l''} + 2E_k(j)E_{l'}(j)\delta_{ll''} \\ &+ 2E_k(j)E_{l''}(j)\delta_{ll'} + 2E_l(j)E_{l'}(j)\delta_{kl''} \\ &+ 2E_l(j)E_{l''}(j)\delta_{kl'} + 2E_{l'}(j)E_{l''}(j)\delta_{kl} \\ &+ E^2(j)\delta_{kl}\delta_{l'l''} + E^2(j)\delta_{kl'}\delta_{ll''} + E^2(j)\delta_{kl''}\delta_{ll'}] \\ &- 6\zeta_k(j)[4E^2(j)E_k(j)E_l(j)\delta_{l'l''} + 4E^2(j)E_k(j)E_{l'}(j)\delta_{ll''} \\ &+ 4E^2(j)E_k(j)E_{l''}(j)\delta_{ll'} + 4E^2(j)E_l(j)E_{l'}(j)\delta_{kl''} \\ &+ 4E^2(j)E_l(j)E_{l''}(j)\delta_{kl'} + 4E^2(j)E_{l'}(j)E_{l''}(j)\delta_{kl} \\ &+ E^4(j)\delta_{kl}\delta_{l'l''} + E^4(j)\delta_{kl'}\delta_{ll''} + E^4(j)\delta_{kl''}\delta_{ll'} \\ &+ 8E_k(j)E_l(j)E_{l'}(j)E_{l''}(j)]\}, \end{aligned} \tag{17}$$

where

$$\alpha_k^*(j) = \sum_r \alpha_{k,r}^*(j), \tag{18}$$

$$\theta_k(j) = \frac{\sum_r \alpha_{k,r}^*(j)\,\theta_r^*(j)}{\sum_r \alpha_{k,r}^*(j)}, \tag{19}$$

$$\xi_k(j) = \frac{\sum_r \alpha_{k,r}^*(j)\,\xi_r^*(j)}{\sum_r \alpha_{k,r}^*(j)}, \tag{20}$$

$$\zeta_k(j) = \frac{\sum_r \alpha_{k,r}^*(j)\,\zeta_r^*(j)}{\sum_r \alpha_{k,r}^*(j)}. \tag{21}$$

For the calculation of the first-, second-, and third-order electronic polarizabilities of the Ba^{2+}, Sr^{2+}, Ti^{4+}, and O^{2-} ions, we use the Slater-type orbitals (see [18]). In order to compute the coefficients $\theta_k(j)$, $\xi_k(j)$, and $\zeta_k(j)$ of a given j-ion, we introduce an anisotropic effective nuclear charge of the core seen by the outer electronic layer for every ion. We then fit its components in such a way that the calculated values of the free electronic polarizabilities $\alpha_1^*(j)$, $\alpha_2^*(j)$, and $\alpha_3^*(j)$ coincide with the measured value of the free electronic polarizability $\alpha^{\exp}(j)$ of the same ion. The free electronic polarizabilities are calculated for $\mathbf{E} = 0$. The effective nuclear charges of the other layers are determined by the Slater rules [21]. These fitted values are reported in table 1 while the values of the measured $\alpha^{\exp}(j)$ and the calculated $\theta_k(j)$, $\xi_k(j)$, and $\zeta_k(j)$ are shown in table 2. Note that unlike in former work, we expand the polarizabilities here up to the third order for the reason that we wish to respect the non-linearities at the film surface as well as those at the film/substrate interface.

Finally, the elements of the first-, second-, and third-order electronic polarizability tensors of the j-ion, which will be used in the next subsection, are deduced from table 2 and the

Table 1. The fitted values of the effective nuclear charges of the outer layers of the constituent ions of $BaTiO_3$ and $SrTiO_3$.

j-ion	Effective nuclear charges	
Ba^{2+}	$Z^{*n(x)}_{5sp} = Z^{*n(y)}_{5sp} = 12.7132$	$Z^{*n(z)}_{5sp} = 16.5572$
Sr^{2+}	$Z^{*n(x)}_{4sp} = Z^{*n(y)}_{4sp} = 12.4807$	$Z^{*n(z)}_{4sp} = 15.2313$
Ti^{4+}	$Z^{*n(x)}_{3sp} = Z^{*n(y)}_{3sp} = 12.9898$	$Z^{*n(z)}_{3sp} = 15.4914$
O^{2-}	$Z^{*n(x)}_{2sp} = Z^{*n(y)}_{2sp} = 3.3351$	$Z^{*n(z)}_{2sp} = 3.9589$

Table 2. The measured free electronic polarizabilities α^{exp} (in $Å^3$) and the calculated values of the coefficients θ_k, ξ_k, and ζ_k (in esu CGS units) of the constituent ions of $BaTiO_3$ and $SrTiO_3$.

j-ion	Ba^{2+}	Sr^{2+}	Ti^{4+}	O^{2-}
$\alpha^{exp}(j)$	1.9460[a]	1.0666[b]	0.1859[a]	2.3940[a]
$\theta_1(j)$	3.9296×10^{-15}	3.0471×10^{-15}	3.0859×10^{-16}	1.5286×10^{-14}
$\theta_2(j)$	3.9296×10^{-15}	3.0471×10^{-15}	3.0859×10^{-16}	1.5286×10^{-14}
$\theta_3(j)$	6.2384×10^{-15}	5.3922×10^{-15}	5.7175×10^{-16}	2.8585×10^{-14}
$\xi_1(j)$	0.6042×10^{-28}	3.5964×10^{-29}	3.3557×10^{-31}	0.8055×10^{-27}
$\xi_2(j)$	0.6042×10^{-28}	3.5964×10^{-29}	3.3557×10^{-31}	0.8055×10^{-27}
$\xi_3(j)$	1.0520×10^{-28}	7.1059×10^{-29}	6.9429×10^{-31}	1.6822×10^{-27}
$\zeta_1(j)$	0.5749×10^{-42}	2.4478×10^{-43}	2.0917×10^{-46}	2.4328×10^{-41}
$\zeta_2(j)$	0.5749×10^{-42}	2.4478×10^{-43}	2.0917×10^{-46}	2.4328×10^{-41}
$\zeta_3(j)$	1.0147×10^{-42}	4.9151×10^{-43}	4.3982×10^{-46}	5.1632×10^{-41}

[a] These free electronic polarizabilities, which are found in [22], correspond to the wavelength $\lambda = 589.3$ nm, it being seen that in their evaluation Slater [22] used the refractive index of cubic $BaTiO_3$ at $\lambda = 589.3$ nm: $n_0 = 2.4$ [23].

[b] The value of α^{exp} for the Sr^{2+} ion used here is fitted to the cubic $SrTiO_3$ single crystals. The fitting procedure consists of using the dipole–dipole approximation described in section 2.2 for computing the refractive index n_0 of the cubic $SrTiO_3$, and then fitting the value of $\alpha^{exp}(Sr^{2+})$ for which the computed value of n_0 coincides with the measured number at 589.3 nm of $n_0 = 2.4$ [23, 24]. Note that in the cubic phase of $SrTiO_3$ which is centrosymmetric paraelectric, the spontaneous local electric field is zero and consequently only the free electronic polarizabilities α^{exp} of the constituent ions enter in the computation of the refractive index, because $\alpha_{kl}(j) = \alpha^{exp}(j)\delta_{kl}$, $\beta_{kll'}(j) = 0$, and $\gamma_{kll'}(j) = 0$ (equations (22)–(24)).

following three relations:

$$\begin{aligned}\alpha_{kl}(j) = \alpha^{exp}(j)\{&\delta_{kl} - \theta_k(j)[E^2(j)\delta_{kl} + 2\,E_k(j)E_l(j)] \\ &+ \xi_k(j)[E^4(j)\delta_{kl} + 4\,E^2(j)E_k(j)E_l(j)] \\ &- \zeta_k(j)[E^6(j)\delta_{kl} + 6\,E^4(j)E_k(j)E_l(j)]\}, \qquad (22)\end{aligned}$$

$$\begin{aligned}\beta_{kll'}(j) = \alpha^{exp}(j)\{&-2\theta_k(j)[E_{l'}(j)\delta_{kl} + E_k(j)\delta_{ll'} + E_l(j)\delta_{kl'}] \\ &+ 4\xi_k(j)[E^2(j)E_{l'}(j)\delta_{kl} + E^2(j)E_k(j)\delta_{ll'} \\ &+ E^2(j)E_l(j)\delta_{kl'} + 2E_k(j)E_l(j)E_{l'}(j)] \\ &- 6\zeta_k(j)[E^4(j)E_{l'}(j)\delta_{kl} + E^4(j)E_k(j)\delta_{ll'} \\ &+ E^4(j)E_l(j)\delta_{kl'} + 4E^2(j)E_k(j)E_l(j)E_{l'}(j)]\}, \qquad (23)\end{aligned}$$

$$\begin{aligned}\gamma_{kll'l''}(j) = \alpha^{exp}(j)\{&-2\theta_k(j)[\delta_{kl}\delta_{l'l''} + \delta_{kl'}\delta_{ll''} + \delta_{kl''}\delta_{ll'}] \\ &+ 4\xi_k(j)[2E_k(j)E_l(j)\delta_{l'l''} + 2E_k(j)E_{l'}(j)\delta_{ll''} \\ &+ 2E_k(j)E_{l''}(j)\delta_{ll'} + 2E_l(j)E_{l'}(j)\delta_{kl''}\end{aligned}$$

$$
\begin{aligned}
&+ 2E_l(j)E_{l''}(j)\delta_{kl'} + 2E_{l'}(j)E_{l''}(j)\delta_{kl} \\
&+ E^2(j)\delta_{kl}\delta_{l'l''} + E^2(j)\delta_{kl'}\delta_{ll''} + E^2(j)\delta_{kl''}\delta_{ll'}] \\
&- 6\zeta_k(j)[4E^2(j)E_k(j)E_l(j)\delta_{l'l''} + 4E^2(j)E_k(j)E_{l'}(j)\delta_{ll''} \\
&+ 4E^2(j)E_k(j)E_{l''}(j)\delta_{ll'} + 4E^2(j)E_l(j)E_{l'}(j)\delta_{kl''} \\
&+ 4E^2(j)E_l(j)E_{l''}(j)\delta_{kl'} + 4E^2(j)E_{l'}(j)E_{l''}(j)\delta_{kl} \\
&+ E^4(j)\delta_{kl}\delta_{l'l''} + E^4(j)\delta_{kl'}\delta_{ll''} + E^4(j)\delta_{kl''}\delta_{ll'} \\
&+ 8E_k(j)E_l(j)E_{l'}(j)E_{l''}(j)]\}. \qquad (24)
\end{aligned}
$$

Analysing the results in table 2, it appears that the oxygen ion which has the highest value of the free electronic polarizability α^{exp} also shows the highest values for the coefficients θ_k, ξ_k, and ζ_k, particularly those along the 3-direction which are almost twice as large compared to the values obtained along the 1- and 2-directions. This means that, compared to those for all other ions, the first-, second-, and third-order electronic polarizabilities of the oxygen ions are affected much more, particularly in the 3-direction. Note that in the following subsection, the local electric field $\mathbf{E}$ will be rewritten as $\mathbf{E}^{\mathrm{loc}}$.

2.2. Dipole–dipole interaction

As mentioned above, our model is based on the dipole–dipole interaction in correlation with the quantum mechanical orbital approximation. The model therefore accounts for the crystalline deformations and the ionic shifts within the film, and also for the possible anisotropy in the first-, second-, and third-order electronic polarizabilities both within the film and at both sides of the $BaTiO_3/SrTiO_3$ interface. The ionic shifts are of utmost importance when modelling the surface and interface properties of a ferroelectric system specifically for thin ferroelectric films as discussed here.

The local field acting on a given site i is given by the Lorentz relation: [25]

$$\mathbf{E}^{\mathrm{loc}}(i) = \mathbf{E}^{\mathrm{ext}} + \sum_j \frac{3(\mathbf{p}_j \cdot \mathbf{r}_j)\mathbf{r}_j - \mathbf{r}_j^2\mathbf{p}_j}{\mathbf{r}_j^5} + \mathbf{E}^{\mathrm{cav}}(i). \qquad (25)$$

In the last equation, $\mathbf{E}^{\mathrm{ext}}$ represents an external electric field that generally holds as $\mathbf{E}^{\mathrm{ext}} = \mathbf{E}^{\mathrm{bias}} + \mathbf{E}^{\mathrm{opt}}$, with $\mathbf{E}^{\mathrm{bias}}$ an electric bias field, and $\mathbf{E}^{\mathrm{opt}}$ the optical field acting on the system. The second term on the right-hand side of equation (25) represents the contribution to the local electric field at the site i considered from the dipole moments of all other ions j existing inside the fictitious spherical cavity of radius R^{cav} centred on i. $\mathbf{E}^{\mathrm{cav}}$ in equation (25) denotes the Lorentz cavity field which is the electric field stemming from polarization charges inside the spherical cavity (as a mathematical fiction) cut out from the specimen with the reference ion i as the centre, as sketched in figure 1 (see the Lorentz cavity inside the bulk in figure 1(1)). The cavity has radius R^{cav} and may be truncated for ions situated closer than R^{cav} to the sample surface (see the cavities in figures 1(2) and 1(3)). Usually the Lorentz cavity field, $\mathbf{E}^{\mathrm{cav}}$, is taken to be $\frac{4\pi}{3}\mathbf{P}$ for an infinite medium with uniform polarization. This expression is not valid near the surface/interface because of the non-uniformity of the dielectric polarization (figures 1(4) and 1(5)) or/and because of the incompleteness of the spherical cavity as sketched in figures 1(2) and 1(3). However, we can show that the k-component of the Lorentz cavity field, $\mathbf{E}^{\mathrm{cav}}$, is given by

$$E_k^{\mathrm{cav}}(i) = \pi \int_0^{\pi} P_k(\theta) f_k^{(\mathrm{c})}(\theta)\, \mathrm{d}\theta \qquad (26)$$

where P_k is the k-component of the polarization at point M (see figure 1(1)). The superscript (c) is used to indicate the direction of the ferroelectric thin film polarization (in this work we

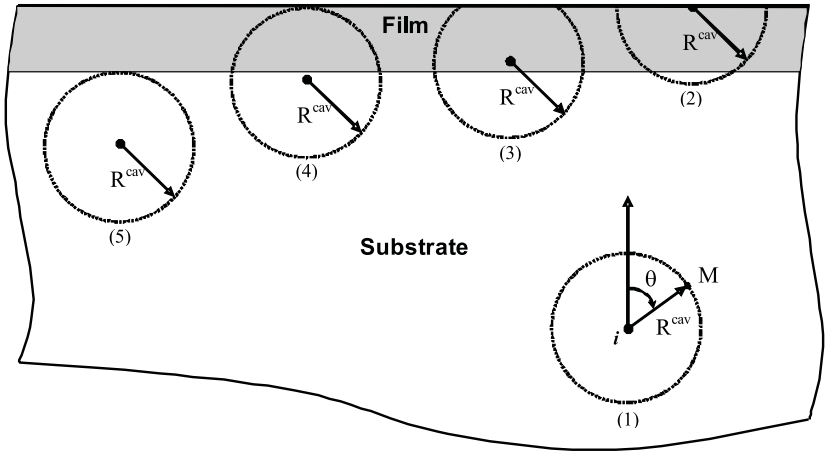

Figure 1. A schematic representation of possible scenarios for Lorentz spherical cavities located near the surface and near the $BaTiO_3/SrTiO_3$ interface.

are interested only in c-oriented $BaTiO_3$ thin films). The function $f_k^{(c)}(\theta)$ is given by (see appendix A)

$$f_k^{(c)}(\theta) = \begin{cases} f_1^{(c)}(\theta) = \sin^3\theta \\ f_2^{(c)}(\theta) = \sin^3\theta \\ f_3^{(c)}(\theta) = 2\sin\theta\cos^2\theta. \end{cases} \tag{27}$$

The k-component of the local electric field acting on the i-ion sitting in the $\tilde{n}(n_x, n_y, n_z)$ unit cell (the indices (n_x, n_y, n_z) represent the coordinates of a unit cell in the whole lattice) is expressed as

$$E_k^{\mathrm{loc}}(\tilde{i}^{\tilde{n}}) = E_k^{\mathrm{ext}} + E_k^{\mathrm{cav}}(\tilde{i}^{\tilde{n}}) + \sum_{j=1}^{5}\sum_{k'=1}^{3}\sum_{\tilde{m}} \frac{3r_{k'}(\tilde{i}^{\tilde{n},\tilde{m}}_{i,j})r_k(\tilde{i}^{\tilde{n},\tilde{m}}_{i,j}) - \delta_{kk'}r^2(\tilde{i}^{\tilde{n},\tilde{m}}_{i,j})}{\|r(\tilde{i}^{\tilde{n},\tilde{m}}_{i,j})\|^5} p_{k'}(\tilde{i}^{\tilde{n},\tilde{m}}_{i,j}) \tag{28}$$

where $\delta_{kk'}$ denotes the Kronecker symbol, and $\mathbf{r}(\tilde{i}^{\tilde{n},\tilde{m}}_{i,j})$ represents the interionic distance between the i-ion in unit cell $\tilde{n}$ and the j-ion in unit cell $\tilde{m}(m_x, m_y, m_z)$. The summation over j and $\tilde{m}$ covers all ions existing inside the sphere of radius R^{cav} centred in the i-ion of the $\tilde{n}$ unit cell. The k-component of the Lorentz cavity electric field at the i-site of the $\tilde{n}$ unit cell is expressed as (see appendix A)

$$E_k^{\mathrm{cav}}(\tilde{i}^{\tilde{n}}) = \sum_{j=1}^{5}\sum_{\tilde{m}} \frac{\pi}{v(\tilde{m})}\left[F_k^{(c)}\left(\arccos\frac{r_3(\tilde{i}^{\tilde{n},\tilde{m}}_{i,1})}{R^{\mathrm{cav}}}\right) - F_k^{(c)}\left(\arccos\frac{r_3(\tilde{i}^{\tilde{n},\tilde{m}+\tilde{1}_c}_{i,1})}{R^{\mathrm{cav}}}\right)\right]\delta_{n_x m_x}\delta_{n_y m_y} p_k(\tilde{i}^{\tilde{n},\tilde{m}}_{i,j}). \tag{29}$$

In the last equation, $v(\tilde{m})$ denotes the volume of the $\tilde{m}$ unit cell, $F_k^{(c)}$ is the primitive function of $f_k^{(c)}$, and $\tilde{m} + \tilde{1}_c$ represents the unit cell $(m_x, m_y, m_z + 1)$. $p_k(\tilde{i}^{\tilde{n},\tilde{m}}_{i,j})$ in equations (28) and (29) is the dipole moment along the k-direction which can be expressed as

$$p_k(\tilde{i}^{\tilde{n},\tilde{m}}_{i,j}) = p_k^{\mathrm{e}}(\tilde{j}^{\tilde{m}}) + p_k^{\mathrm{i}}(\tilde{i}^{\tilde{n},\tilde{m}}_{i,j}), \tag{30}$$

with the two contributions $p_k^{\mathrm{e}}(\tilde{j}^{\tilde{m}})$ and $p_k^{\mathrm{i}}(\tilde{i}^{\tilde{n},\tilde{m}}_{i,j})$ specifying, respectively, the electronic dipole moment and the relative ionic dipole moment in the k-direction of the j-ion located in the $\tilde{m}$

unit cell as seen by the i-ion located in the $\tilde{n}$ unit cell. These dipole moments are calculated up to a third-order development as

$$p_k^{\mathrm{e}}(\tilde{m}_j) = \sum_{l=1}^{3} \alpha_{kl}^{\mathrm{eff}}(\tilde{m}_j) E_l^{\mathrm{loc}}(\tilde{m}_j) + \tfrac{1}{2} \sum_{l=1}^{3}\sum_{l'=1}^{3} \beta_{kll'}^{\mathrm{eff}}(\tilde{m}_j) E_l^{\mathrm{loc}}(\tilde{m}_j) E_{l'}^{\mathrm{loc}}(\tilde{m}_j) + \tfrac{1}{6} \sum_{l=1}^{3}\sum_{l'=1}^{3}\sum_{l''=1}^{3} \gamma_{kll'l''}^{\mathrm{eff}}(\tilde{m}_j) E_l^{\mathrm{loc}}(\tilde{m}_j) E_{l'}^{\mathrm{loc}}(\tilde{m}_j) E_{l''}^{\mathrm{loc}}(\tilde{m}_j) \tag{31}$$

and

$$p_k^{\mathrm{i}}(\tilde{n}_{i,j}, \tilde{m}) = \sum_{l=1}^{3} Z_{kl}^{*\mathrm{s}}(\tilde{m}_j)\, e\, [s_l(\tilde{m}_j) - s_l(\tilde{n}_i)]. \tag{32}$$

In equation (31), $\alpha_{kl}^{\mathrm{eff}}(\tilde{m}_j)$, $\beta_{kll'}^{\mathrm{eff}}(\tilde{m}_j)$, and $\gamma_{kll'l''}^{\mathrm{eff}}(\tilde{m}_j)$ represent, respectively, the (kl) element of the first-order effective electronic polarizability tensor, the (kll') element of the second-order effective electronic polarizability tensor, and the $(kll'l'')$ element of the third-order effective electronic polarizability tensor of the j-ion located in the $\tilde{m}$ unit cell, given by equations (B.7)–(B.9) in appendix B. In equation (32), $Z_{kl}^{*\mathrm{s}}(\tilde{m}_j)$ denotes the (kl) component of the static effective charge tensor of the j-ion located in the $\tilde{m}$ unit cell as given at the beginning of section 3, and $s_l(\tilde{n}_i)$ and $s_l(\tilde{m}_j)$ denote the shifts along the l-direction, respectively, of the i- and j-ions located, respectively, in the $\tilde{n}$ and $\tilde{m}$ unit cells. Thus the local electric field present along the k-direction acting on ion i of the $\tilde{n}$ unit cell can be written as

$$\sum_{j=1}^{5}\sum_{l=1}^{3}\sum_{\tilde{m}} S_{kl}(\tilde{n}_{i,j}, \tilde{m}) E_l^{\mathrm{loc}}(\tilde{m}_j) = Q_k(\tilde{n}_i), \tag{33}$$

with

$$S_{kl}(\tilde{n}_{i,j}, \tilde{m}) = \delta_{kl}\delta_{ij}\delta_{\tilde{n}\tilde{m}} - \sum_{k'=1}^{3} T_{kk'}(\tilde{n}_{i,j}, \tilde{m})[\alpha_{k'l}^{\mathrm{eff}}(\tilde{m}_j) + \sigma_{k'l}^{\mathrm{eff}}(\tilde{m}_j) + \rho_{k'l}^{\mathrm{eff}}(\tilde{m}_j)], \tag{34}$$

and

$$Q_k(\tilde{n}_i) = E_k^{\mathrm{ext}} + \sum_{j=1}^{5}\sum_{k'=1}^{3}\sum_{\tilde{m}} T_{kk'}(\tilde{n}_{i,j}, \tilde{m})\, p_{k'}^{\mathrm{i}}(\tilde{n}_{i,j}, \tilde{m}), \tag{35}$$

where

$$T_{kk'}(\tilde{n}_{i,j}, \tilde{m}) = \frac{3r_{k'}(\tilde{n}_{i,j}, \tilde{m}) r_k(\tilde{n}_{i,j}, \tilde{m}) - \delta_{kk'} r^2(\tilde{n}_{i,j}, \tilde{m})}{\|\mathbf{r}(\tilde{n}_{i,j}, \tilde{m})\|^5} + \frac{\pi}{v(\tilde{m})}\left[F_{k'}^{(\mathrm{c})}\left(\arccos\frac{r_3(\tilde{n}_{i,1}, \tilde{m})}{R^{\mathrm{cav}}}\right) - F_{k'}^{(\mathrm{c})}\left(\arccos\frac{r_3(\tilde{n}_{i,1}, \tilde{m}+\tilde{1}_{\mathrm{c}})}{R^{\mathrm{cav}}}\right)\right]\delta_{n_x m_x}\delta_{n_y m_y}\delta_{kk'}, \tag{36}$$

$$\sigma_{k'l}^{\mathrm{eff}}(\tilde{m}_j) = \tfrac{1}{2}\sum_{l'=1}^{3} \beta_{k'll'}^{\mathrm{eff}}(\tilde{m}_j) E_{l'}^{\mathrm{loc}}(\tilde{m}_j), \tag{37}$$

and

$$\rho_{k'l}^{\mathrm{eff}}(\tilde{m}_j) = \tfrac{1}{6}\sum_{l'=1}^{3}\sum_{l''=1}^{3} \gamma_{k'll'l''}^{\mathrm{eff}}(\tilde{m}_j) E_{l'}^{\mathrm{loc}}(\tilde{m}_j) E_{l''}^{\mathrm{loc}}(\tilde{m}_j). \tag{38}$$

The second-rank tensors $\tilde{\sigma}^{\mathrm{eff}}(\tilde{m}_j)$ and $\tilde{\rho}^{\mathrm{eff}}(\tilde{m}_j)$ are introduced in order to represent, respectively, the effect of the second-order effective electronic polarizability $\tilde{\beta}^{\mathrm{eff}}(\tilde{m}_j)$ tensor

(third-rank tensor) and the third-order effective electronic polarizability $\tilde{\gamma}^{\mathrm{eff}}(\tilde{m}_j)$ tensor (fourth-rank tensor).

From equations (33) and (34) it appears that the components of the local electric field depend on those of the first-, second-, and third-order effective electronic polarizabilities, while these, in turn, also depend on the electric field components through equations (B.7)–(B.9), (22)–(24). This mutual dependence between the first-, second-, and third-order electronic polarizabilities (orbital approximation), on one hand, and their dependence on the electric field (dipole–dipole interaction), on the other hand, make a self-consistent calculation necessary.

By solving equation (33) we obtain $E_l^{\mathrm{loc}}(\tilde{m}_j)$, the l-component of the local electric field of the j-ion located in the $\tilde{m}$ unit cell. The total polarization, $P_k(\tilde{m})$, of the $\tilde{m}$ unit cell is expressed as

$$P_k(\tilde{m}) = \frac{1}{v(\tilde{m})} \sum_{j=1}^{5} \left[p_k^{\mathrm{e}}(\tilde{m}_j) + \sum_{l=1}^{3} Z_{kl}^{*\mathrm{s}}(\tilde{m}_j)\, e \cdot s_l(\tilde{m}_j) \right]. \tag{39}$$

The connection between the optical dielectric constant $\varepsilon_{kl'}^{\mathrm{opt}}(\tilde{m})$, electronic dipole moments $p_k^{\mathrm{e}}(\tilde{m}_j)$, and the optical electric field $E_{l'}^{\mathrm{opt}}$ is expressed in the following way:

$$\varepsilon_{kl'}^{\mathrm{opt}}(\tilde{m}) = \delta_{kl'} + \frac{4\pi}{v(\tilde{m})} \sum_{j=1}^{5} \frac{\partial p_k^{\mathrm{e}}(\tilde{m}_j)}{\partial E_{l'}^{\mathrm{opt}}}. \tag{40}$$

Using equation (31), the term $\frac{\partial p_k^{\mathrm{e}}(\tilde{m}_j)}{\partial E_{l'}^{\mathrm{opt}}}$ can be written as

$$\frac{\partial p_k^{\mathrm{e}}(\tilde{m}_j)}{\partial E_{l'}^{\mathrm{opt}}} = \sum_{l=1}^{3} [\alpha_{kl}^{\mathrm{eff}}(\tilde{m}_j) + 2\,\sigma_{kl}^{\mathrm{eff}}(\tilde{m}_j) + 3\,\rho_{kl}^{\mathrm{eff}}(\tilde{m}_j)] \frac{\partial E_l^{\mathrm{loc}}(\tilde{m}_j)}{\partial E_{l'}^{\mathrm{opt}}}. \tag{41}$$

Note that $\frac{\partial E_l^{\mathrm{loc}}(\tilde{m}_j)}{\partial E_{l'}^{\mathrm{opt}}}$, which represents the local electric field induced along the l-direction of the j-ion located in the $\tilde{m}$ unit cell by unit of the l'-component of the optical electric field, is obtained by solving the following equation, deduced from equation (28):

$$\sum_{j=1}^{5} \sum_{l=1}^{3} \sum_{\tilde{m}} S_{kl}^{*}(\tilde{n},\tilde{m}_{i,j}) \frac{\partial E_l^{\mathrm{loc}}(\tilde{m}_j)}{\partial E_{l'}^{\mathrm{opt}}} = \delta_{kl'}, \tag{42}$$

where

$$S_{kl}^{*}(\tilde{n},\tilde{m}_{i,j}) = \delta_{kl}\delta_{ij}\delta_{\tilde{n}\tilde{m}} - \sum_{k'=1}^{3} T_{kk'}(\tilde{n},\tilde{m}_{i,j})[\alpha_{k'l}^{\mathrm{eff}}(\tilde{m}_j) + 2\,\sigma_{k'l}^{\mathrm{eff}}(\tilde{m}_j) + 3\,\rho_{k'l}^{\mathrm{eff}}(\tilde{m}_j)]. \tag{43}$$

In electromagnetic theory [26] the refractive index of light polarized along the k-direction of the $\tilde{m}$ unit cell is given by

$$n_k(\tilde{m}) = \frac{1}{\sqrt{\eta_{kk}^{\mathrm{opt}}(\tilde{m})}}. \tag{44}$$

where $\tilde{\eta}^{\mathrm{opt}}(\tilde{m})$ represents the optical dielectric impermeability tensor of the $\tilde{m}$ unit cell $\tilde{\eta}^{\mathrm{opt}}(\tilde{m}) = (\tilde{\varepsilon}^{\mathrm{opt}}(\tilde{m}))^{-1}$.

3. Results and discussion

The calculation of the spontaneous polarization and refractive indices is carried out for two different thicknesses (i.e. 10 and 20 ML; ML = monolayer) of *c*-oriented thin films of $BaTiO_3$ on the $SrTiO_3$ substrate at room temperature. In this calculation we take into account that the lattice parameter of the substrate, which has a cubic structure, is $a = 3.905$ Å, the spontaneous ionic shifts are zero, and the static effective charges are [27] $Z^{*s}_{kk}(Sr^{2+}) = 1.852$, $Z^{*s}_{kk}(Ti^{4+}) = 2.272$, and $Z^{*s}_{kk}(O^{2-}_{x,y,z}) = -1.375$ (the charge neutrality sum rule is fulfilled to 1‰: $\sum_{j=1}^{5} Z^{*s}(j) = -0.001$). The $BaTiO_3$ thin film undergoes a lattice strain by keeping its tetragonal structure [4, 7]. The lattice parameters of the thin film are $a = b = 3.905$ Å (coinciding with that of the $SrTiO_3$ substrate) and $c = \frac{v^{blk}}{ab}$ (v^{blk} is the volume of the bulk unit cell in $BaTiO_3$) [4, 7], and the spontaneous ionic shifts are [18, 28] $s_3(Ba^{2+}) = 0$ Å, $s_3(Ti^{4+}) = 0.05$ Å, $s_3(O^{2-}_{x,y}) = -0.05$ Å, and $s_3(O^{2-}_{z}) = -0.09$ Å. As static effective charges of the film, we use the data published in a recent theoretical work devoted to the quantitative study of successive phase transitions in $BaTiO_3$ [29–31]: $Z^{*s}_{33}(Ba^{2+}) = 1.437$, $Z^{*s}_{33}(Ti^{4+}) = 2.063$, $Z^{*s}_{33}(O^{2-}_{x,y}) = -1.200$, and $Z^{*s}_{33}(O^{2-}_{z}) = -1.100$. It is noteworthy that for symmetry reasons the static effective charge tensors of the constituent ions of both cubic $SrTiO_3$ and tetragonal $BaTiO_3$ have to be diagonal and consequently the non-diagonal elements Z^{*s}_{kl} are zero. The in-plane lattice parameters considered here for the thin film of 20 ML thickness are slightly different from those published by Yoneda *et al* [4, 7]. In fact, for simplifying the modelling, it is very important to assume that the in-plane lattice parameters of the $BaTiO_3$ film coincide exactly with those of the $SrTiO_3$ substrate, because the mismatch between the in-plane lattice parameters of the film and the substrate generates dislocations in the crystallographic structure of the film and then renders the modelling very complicated. However, the unit cell volume is independent of the film thickness for $BaTiO_3$ ultrathin films at room temperature as shown experimentally by Yoneda *et al* [4, 7]. It is also assumed that these magnitudes (lattice parameters, static effective charges, and ionic shifts) are valid both near the surface/interface and in the bulk. In our computation we have to solve equations (33) and (42) which are, in fact, two sets of equations. By considering only the 86 unit cell monolayers nearest to the surface and taking into account that all unit cells in the same monolayer have the same properties, the number of equations in each set can be reduced to $3 \times 5 \times 86 = 1290$ equations. The wavelength at which our optical properties (i.e. the refractive indices and optical birefringence) have been computed is $\lambda = 589.3$ nm, purposely chosen to coincide with the availability of literature data for the free electronic polarizabilities. Treating the full spectral response of the coupled $SrTiO_3/BaTiO_3$ system would need the Schrödinger equation to be solved time dependently, which is beyond the scope of this paper.

Before presenting and discussing the results obtained for the spontaneous polarization and refractive indices of the thin films, we would first like to draw attention to the impact of the non-linearity in the electronic polarizabilities as well as of the lattice strain on the magnitudes of interest (i.e. the spontaneous polarization and refractive indices) of $BaTiO_3$ and $SrTiO_3$ single crystals.

3.1. $BaTiO_3$ and $SrTiO_3$ single crystals

In this subsection, which is restricted to the room temperature tetragonal $BaTiO_3$ and cubic $SrTiO_3$ single crystals, we present and discuss the dependence of the electrical and optical properties on some magnitudes used in this model such as the order of the electronic polarizability taken into account in the calculation and also the lattice strain. As shown in the theoretical formalism presented in the previous section, our model takes into account

Table 3. The spontaneous polarization (in C m^{-2}), refractive indices, and optical birefringence of $BaTiO_3$ single crystals at 589.3 nm and room temperature calculated as functions of the orders of the electronic polarizabilities. Measured values are also reported for comparison.

Electronic polarizabilities	P^{spn}	n_{o}	n_{e}	δn
No polarizability[a]	0.0802[b]	1[c]	1[c]	0
First order[d]	0.2536	2.3854	2.3153	−0.0702
First and second order[e]	0.2820	2.3846	2.3140	−0.0706
First to third order[f]	0.2771	2.3848	2.3150	−0.0698
Measured values	0.2800[g]	2.3700[h]	2.3120[h]	−0.0580[h]

[a] Here, all orders of the electronic polarizability are ignored and then the ions are considered as rigid (non-polarizable).
[b] This value represents the ionic contribution to the spontaneous polarization.
[c] The refractive index of the non-polarizable medium coincides with that of the vacuum.
[d] In this case only the first-order electronic polarizability ($\tilde{\alpha}$) is considered. The terms with ξ and ζ in the expression for $\alpha_{kl}(j)$ (equation (22)) are omitted.
[e] In this case the first-order ($\tilde{\alpha}$) and second-order ($\tilde{\beta}$) electronic polarizabilities are considered. The terms with ζ in the expression of $\alpha_{kl}(j)$ (equation (22)) and $\beta_{kll'}(j)$ (equation (23)) are omitted.
[f] In this case all three orders of the electronic polarizabilities ($\tilde{\alpha}$, $\tilde{\beta}$ and $\tilde{\gamma}$) are considered.
[g] Reference [32].
[h] These optical values, which are found in [23], are measured at room temperature and wavelength $\lambda = 589.3$ nm.

the effects of both the first-, second-, and third-order electronic polarizabilities. In order to study the contributions of each of these linear and non-linear electronic polarizabilities, we report in table 3 the calculated values of the spontaneous polarization, refractive indices, and optical birefringence of $BaTiO_3$ single crystals at room temperature for different orders of expansion of the electronic polarizabilities. From these results, it appears that the main contributor to the optical properties of $BaTiO_3$ is the first-order electronic polarizability. For the spontaneous polarization, in which the ionic polarization contributes 28.94%, the first-, second-, and third-order electronic polarizabilities contribute, respectively, 62.58%, 10.25%, and −1.77%. The fact that the contribution of the third-order electronic polarizability to the spontaneous polarization is lower than 2% (in absolute numbers) means that the expansion of the electronic polarizabilities up to the third order is enough for obtaining accurate results for both electrical and optical properties of $BaTiO_3$. It is noteworthy that our theoretically computed values of the dielectric spontaneous polarizations, refractive indices, and optical birefringence agree well with the measured ones. For the room temperature cubic $SrTiO_3$ single crystals the dielectric spontaneous polarization as well as the spontaneous local electric field are zero. However, the lone contributor of the optical properties of the medium, which are isotropic ($n = 2.4$), is the first-order electronic polarizability tensor $\tilde{\alpha}$, of which only the diagonal elements are non-zero and coincide with the free electronic polarizability α^{exp} (equation (22)). The second- and third-order electronic polarizabilities are exactly zero (equations (23) and (24)) and the medium does not present any non-linearity.

Among the magnitudes upon which the electrical and optical properties strongly depend are the lattice parameters which, under mechanical strain as in thin films, show an important deviation from those of the bulk single crystals in the spontaneous state. In order to show the influence of the change of the lattice parameters on the spontaneous polarization, refractive indices, and optical birefringence, we report in table 4 some sets of the lattice parameters of both $BaTiO_3$ and $SrTiO_3$ single crystals, and the corresponding calculated values of the above-mentioned magnitudes at room temperature. The data for the spontaneous ionic shifts and ionic static effective charges used in the calculation are the same as those given at the

Table 4. The spontaneous polarization (in C m^{-2}), refractive indices, and optical birefringence of $BaTiO_3$ and $SrTiO_3$ single crystals at 589.3 nm and room temperature calculated using various sets of lattice parameters.

		The parameters		The calculated magnitudes			
Material	Structure	a	c	P^{spn}	n_o	n_e	δn
$BaTiO_3$	Tetragonal	3.9920[a]	4.0350[a]	0.2771	2.3848	2.3150	−0.0698
$BaTiO_3$	Tetragonal	3.9050[b]	4.2168[b]	0.2181	2.4236	2.2945	−0.1291
$SrTiO_3$	Cubic	3.9050[c]		0	2.4000	2.4000	0
$SrTiO_3$	Tetragonal	3.9920[d]	3.7366[d]	0	2.3711	2.4794	0.1082

[a] This is the set of room temperature single-crystal $BaTiO_3$ measured lattice parameters [17].
[b] This set of lattice parameters of tetragonal $BaTiO_3$ is chosen in such a way that the a lattice parameter coincides with that of cubic $SrTiO_3$ and the unit cell volume coincides with that measured for the $BaTiO_3$ single crystals, i.e. $v^{blk} = 64.302$ Å^3 [4, 17].
[c] This is the set of room temperature single-crystal $SrTiO_3$ measured lattice parameters [5].
[d] This set of lattice parameters of *tetragonal* $SrTiO_3$ is chosen in such a way that the a lattice parameter coincides with that of tetragonal $BaTiO_3$ and the unit cell volume coincides with that measured for the $SrTiO_3$ single crystals, i.e. $v^{blk} = 59.547$ Å^3 [5].

beginning of this section. We see that the elongation of the tetragonal $BaTiO_3$ unit cell in the 3-direction causes an important change of the spontaneous polarization. It decreases from 0.2771 to 0.2181 C m^{-2} when the c lattice parameter increases from 4.0350 to 4.2168 Å. The refractive indices, in turn, undergo a change which is manifested in an increase of the ordinary refractive index (from 2.3848 to 2.4236) and a decrease of the extraordinary refractive index (from 2.3150 to 2.2945). Moreover, the optical birefringence of $BaTiO_3$, which remains a uniaxial negative material, increases in absolute numbers from 0.0698 to 0.1291. In fact, the elongation of the $BaTiO_3$ unit cell in the 3-direction, which is accompanied with a shortening of the unit cell in the 1- and 2-directions, causes a decrease of the spontaneous local electric field of the constituent ions and then an increase of their first-order electronic polarizabilities (the main contributor to the optical properties as shown at the beginning of this subsection). However, the change of the refractive indices results from:

- The effect of the elongation of the unit cell in the 3-direction, which causes the decrease of the refractive index polarized in the same direction (i.e. n_e), and the shortening of the unit cell in the other directions, which causes the increase of the refractive index polarized in those directions (i.e. n_o).
- The effect of the first-order electronic polarizabilities of the constituent ions which is manifested in an increase of all refractive indices.

It appears that the main reason why the change undergone by the ordinary refractive index n_o is larger than that undergone by the extraordinary refractive index n_e (even though the elongation in the 3-direction is larger than the shortening in the other directions) is the fact that the increase of n_o results from the cooperation of the two above-mentioned effects while the change of n_e results from their competition (because they have opposite signs).

For $SrTiO_3$, the transformation of the unit cell from cubic to tetragonal structure (table 4) has no effect on the spontaneous polarization which, as the spontaneous ionic shifts, remains zero. In fact, the generator of the spontaneous polarization in the ferroelectric perovskite materials is the spontaneous ionic shifts rather than the crystalline deformation. However, the crystalline deformations (elongation and shortening) contribute to the change of the spontaneous polarization, as shown in the previous paragraph, but they do not generate it. The shortening of the $SrTiO_3$ unit cell in one direction and its elongation in the other directions

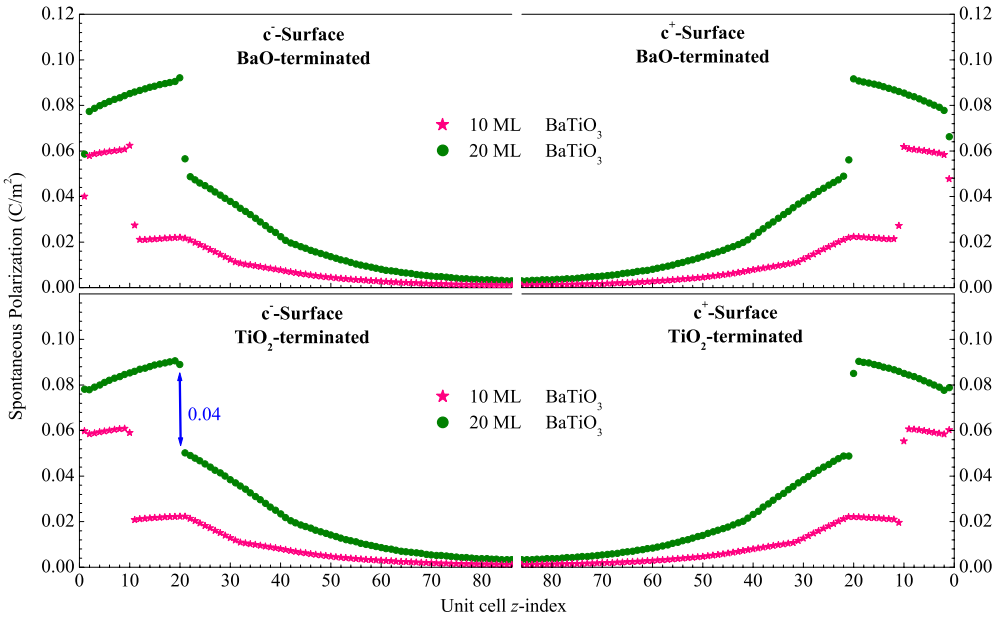

Figure 2. Variation of the spontaneous polarization within the $BaTiO_3$ ultrathin film (both BaO- and TiO_2-terminated surfaces) and the $SrTiO_3$ substrate. Results are computed at room temperature for two different values of the film thickness, 10 and 20 ML. The Lorentz spherical cavity radius measures $R^{\mathrm{cav}} = 80$ Å.

strongly affect the refractive indices. In fact, $SrTiO_3$, which is optically isotropic in the cubic phase, becomes anisotropic uniaxial positive ($\delta n > 0$) material after the shortening of one of its lattice parameters. Yet the change undergone by the extraordinary refractive index of the light polarized in the shortening direction n_{e}, which increases from 2.4 to 2.4794, is more than double (in absolute numbers) that undergone by the ordinary refractive index of the light polarized in the elongation directions n_{o}, which decreases from 2.4 to 2.3711. This result can be explained by the fact that the shortening of the c lattice parameter of the unit cell is larger than the elongation of its a lattice parameter (see table 4).

3.2. $BaTiO_3$ thin films on $SrTiO_3$ substrate

Now we present and discuss the results obtained for the spontaneous polarization in the $\tilde{n}$ unit cell, $P^{\mathrm{spn}}(\tilde{n})$. $P^{\mathrm{spn}}(\tilde{n})$ is ascribed to the unit cell (and not to individual ions) and is defined as the total dipole moment (in the unit cell) per volume. The components $P_k(\tilde{n})$ are deduced from equation (39) in the absence of any external field. The calculation shows that the values of the spontaneous polarization within the $SrTiO_3$ substrate and the $BaTiO_3$ ultrathin film at room temperature along the 1- and 2-directions are exactly zero. On the other hand, the 3-component of the spontaneous polarization $P_3^{\mathrm{spn}}(\tilde{n})$ is non-zero and is displayed in figure 2 for the two film thicknesses of 10 and 20 ML (calculated for both BaO- and TiO_2-terminated surfaces). We see that, for each thickness of the film, the behaviours of the spontaneous polarization near the c-surface/interface are the same for the four cases distinguished here ($c^{\pm}$-surfaces, both BaO and TiO_2 terminated). However, two differences distinguish the film with the BO-terminated surface from that with TiO_2 termination. The first one is manifested in the effective value of the spontaneous polarization of the $BaTiO_3$ unit cell monolayer closest

to the surface, which is smaller for BaO-terminated surfaces (both c^-- and c^+-surfaces) than for TiO_2-terminated surfaces (both c^-- and c^+-surfaces). The second aspect concerns the effective value of the spontaneous polarization of the $SrTiO_3$ unit cell monolayer closest to the interface which is larger for BaO-terminated surfaces (both c^-- and c^+-surfaces) than for TiO_2-terminated surfaces (both c^-- and c^+-surfaces). Yet, in all cases the spontaneous polarization of the film increases when its thickness increases, achieving values of $\sim$0.060 and $\sim$0.085 C m^{-2} (mean values) for 10 and 20 ML of $BaTiO_3$ on $SrTiO_3$. Moreover, the value of the spontaneous polarization within the film always decreases when approaching the surface. This decrease is mainly attributed to the surface effect, because the closer the ion is to the $BaTiO_3$ surface, the more incomplete the spherical cavity is, resulting in a smaller number of ions interacting with the ion considered. It has been shown, in a recent experimental work, that the magnitude of the spontaneous polarization of $BaTiO_3$ film of 30 ML thickness is around 0.03 C m^{-2} [4] which is smaller than that estimated from our calculation. This difference might be attributed to the depolarizing electric field induced within the film by the surface and interface charges [33, 34].

It appears that not only the $BaTiO_3$ film, but also the $SrTiO_3$ substrate has a dielectric spontaneous polarization. This polarization is important near the $BaTiO_3$/$SrTiO_3$ interface and decreases to zero far into the bulk. It is purely electronic because the ionic polarization is zero within the $SrTiO_3$ substrate (the substrate ionic polarization is zero because the ionic shifts are zero). We notice that the spontaneous polarization generated within the substrate is induced, through the dipolar interactions, by the dipole moments (polarized ions) existing within the film. It remains to note that the gap in the spontaneous polarization seen at the interface is due to the vanishing of the ionic polarization when passing from the $BaTiO_3$ film to the substrate. As seen in figure 2, this polarization difference is almost independent of the film thickness and has a value of $\sim$0.04 C m^{-2}.

Figure 3 reports the calculated values for the refractive indices ascribed to each unit cell within the $SrTiO_3$ substrate and the $BaTiO_3$ ultrathin films (both BaO- and TiO_2-terminated surfaces) at room temperature for the two different thicknesses considered. Note that the calculated results are displayed as discrete values for the refractive indices, making sense on unit cell bases only (and not on the ionic scale). For both thicknesses of the ultrathin film (either BaO- or TiO_2-terminated surfaces), the n_3 refractive index, which corresponds to light polarized perpendicular to the surface/interface, undergoes a very strong decrease when approaching the surface without showing any discontinuity at the interface as is the case for the spontaneous polarization. Values range from 2.4 (which is the refractive index of the bulk of $SrTiO_3$) inside the substrate (far away from the surface) to $\sim$1.75 close to the surface. However, the change undergone by the refractive indices n_1 and n_2 (which coincide with each other; i.e. $n_1 = n_2$), corresponding to light polarized in the plane parallel to the surface/interface, is very small. This change is manifested in a variation in both refractive indices near the surface accompanied by a small discontinuity at the interface.

In all cases studied, the refractive indices corresponding to light polarized parallel to the surface (i.e. n_1 and n_2) of the unit cell monolayer closest to the sample surface are slightly smaller than those of the other unit cell monolayers.

Far away from the surface into the $SrTiO_3$ bulk, whatever the thickness of the film, the medium becomes isotropic as it possesses only one refractive index which coincides with that of the bulk of cubic $SrTiO_3$ single crystals ($n_0 = 2.4$) [23, 24]. Nevertheless, the sample behaves near the surface like a uniaxial negative material with a high optical birefringence of $\delta n \sim 0.6$.

Our theoretical calculations show that the spontaneous polarization increases with the thickness of the thin film while the behaviour of the refractive indices is almost the same whatever the thickness of the film. The spontaneous polarization is always parallel to the

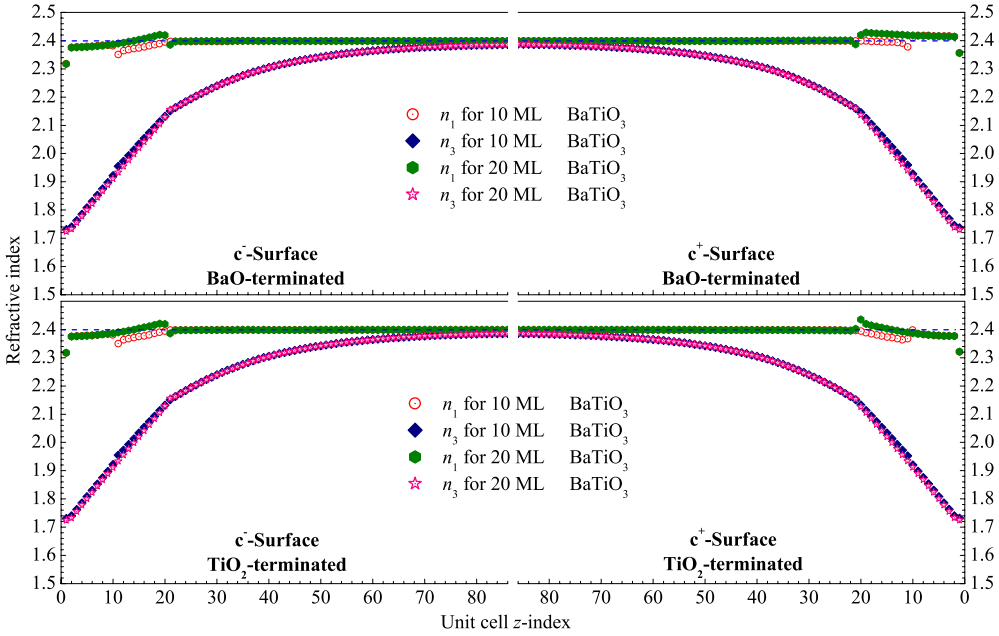

Figure 3. The variation of the refractive indices within the $BaTiO_3$ ultrathin film (both BaO- and TiO_2-terminated surfaces) and the $SrTiO_3$ substrate. Results are computed at room temperature for two different values of the film thickness, 10 and 20 ML. The Lorentz spherical cavity radius is $R^{\mathrm{cav}} = 80$ Å. The dashed line represents the measured value of the refractive index of $SrTiO_3$ single crystals at 589.3 nm and room temperature according to Levin *et al* [23, 24].

c-axis and its value decreases strongly when crossing the interface from the film towards the substrate. On the other hand, the refractive index corresponding to light polarized perpendicular to the sample surface undergoes an important change near the surface.

4. Conclusions

By using a microscopic model taking into account a quantum method based upon the orbital approximation and the dipole–dipole interaction due to the local electric field acting on the constituent ions, we calculated the electric and optical properties near the surface and interface of *c*-oriented ultrathin films of $BaTiO_3$ on a $SrTiO_3$ substrate at room temperature. The calculations show that the spontaneous polarization of the film increases with its thickness, as does that of the substrate in the neighbourhood of the interface, while the refractive index behaviour remains almost the same on changing the thickness of the film. However, the magnitude of the spontaneous polarization of an ultrathin film of $BaTiO_3/SrTiO_3$ is smaller than that for tetragonal $BaTiO_3$ single crystals, indicating that the lattice strain and the surface/interface effects present induced polarization suppression as observed by Yoneda *et al* in recent experimental work [4]. Moreover, the spontaneous polarization of the $BaTiO_3$ film decreases near the surface and behaves quite similarly to what was found in recent theoretical work based on Landau [33, 35] and Landau–Ginzburg–Devonshire thermodynamic theory [36] and also from shell model calculations for ultrathin films [37]. Furthermore, the $BaTiO_3/SrTiO_3$ ultrathin film behaves like a uniaxial crystal, resulting in dramatic changes of the refractive index n_3 near the surface/interface. Far away from the surface/interface the

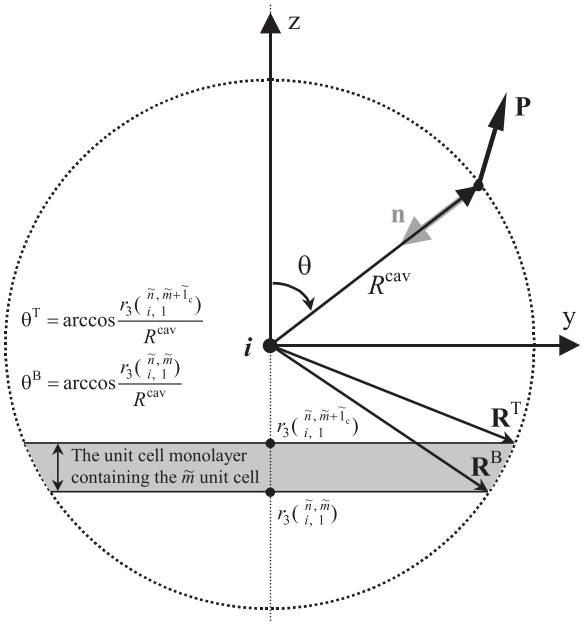

Figure A.1. A schematic representation of the Lorentz spherical cavity for the *c*-surface/interface. $r_3(\tilde{i}_{,1}^{\tilde{n},\tilde{m}})$ and $r_3(\tilde{i}_{,1}^{\tilde{n},\tilde{m}+\tilde{1}_c})$ are, respectively, the bottom and top edges of the unit cell monolayer containing the $\tilde{m}$ unit cell. θ^B and θ^T are, respectively, the angles between the z-axis, on one hand, and the vectors $\mathbf{R}^B$ and $\mathbf{R}^T$, on the other hand. The centre i coincides with the i-ion of the $\tilde{n}$ unit cell.

material becomes isotropic. This effect might be the main origin of the reduction of the refractive indices of $BaTiO_3$ films observed in recent experimental work [8, 11].

Acknowledgments

Financial support of this work by the 'Deutsche Forschungsgemeinschaft' under grants Nos EN 434/7, EN 434/2, and EN 434/14 is gratefully acknowledged.

Appendix A. The Lorentz cavity field expression

The development of the expression for the local electric field created by the spherical Lorentz cavity will be demonstrated, in this appendix, for the *c*-surface/interface. However, near the *c*-surface/interface, the polarization **P** on the Lorentz cavity surface is not uniform and depends on z (or θ, when using spherical coordinates). The element of the electric field created in the centre i (see figure A.1) by the charges located in the area element d**S** with

$$\mathrm{d}\mathbf{S} = (R^{cav})^2 \sin\theta \, \mathrm{d}\theta \, \mathrm{d}\varphi \cdot \mathbf{n} \tag{A.1}$$

is denoted as

$$\delta\mathbf{E}^{cav} = (\mathbf{P} \cdot \mathbf{n}) \cdot \sin\theta \, \mathrm{d}\theta \, \mathrm{d}\varphi \cdot \mathbf{n}. \tag{A.2}$$

n is the unit vector normal to the surface and the product $\mathbf{P} \cdot \mathbf{n}$ represents the charge density in the area element d**S**.

By taking into account that the polarization depends only on θ, the components of $\delta\mathbf{E}^{\mathrm{cav}}$ can be expressed as

$$\begin{aligned}\delta E_1^{\mathrm{cav}} &= \pi P_1(\theta)\sin^3\theta\,\mathrm{d}\theta\\ \delta E_2^{\mathrm{cav}} &= \pi P_2(\theta)\sin^3\theta\,\mathrm{d}\theta\\ \delta E_3^{\mathrm{cav}} &= 2\pi P_3(\theta)\sin\theta\cos^2\theta\,\mathrm{d}\theta.\end{aligned} \tag{A.3}$$

Thus

$$E_k^{\mathrm{cav}} = \pi\int_0^{\pi} P_k(\theta) f_k^{(\mathrm{c})}(\theta)\,\mathrm{d}\theta \tag{A.4}$$

with

$$f_k^{(\mathrm{c})}(\theta) = \begin{cases} f_1^{(\mathrm{c})}(\theta) = \sin^3\theta\\ f_2^{(\mathrm{c})}(\theta) = \sin^3\theta\\ f_3^{(\mathrm{c})}(\theta) = 2\sin\theta\cos^2\theta.\end{cases} \tag{A.5}$$

Now, let us assume that the polarization $\mathbf{P}$ is constant over each unit cell monolayer, $\mathbf{P}$ is constant between $r_3(\tilde{i}_{,1}^{\tilde{n},\tilde{m}})$ and $r_3(\tilde{i}_{,1}^{\tilde{n},\tilde{m}+\tilde{1}_{\mathrm{c}}})$ (see figure A.1). Therefore, the k-component of the Lorentz cavity electric field of the i-ion in the $\tilde{n}$ unit cell can be computed as

$$\begin{aligned}E_k^{\mathrm{cav}}(\tilde{i}^{\tilde{n}}) &= \pi\sum_{m_z} P_k(^{m_z})\int_{\theta^{\mathrm{T}}}^{\theta^{\mathrm{B}}} f_k^{(\mathrm{c})}(\theta)\,\mathrm{d}\theta\\ &= \pi\sum_{\tilde{m}} P_k(^{\tilde{m}})[F_k^{(\mathrm{c})}(\theta^{\mathrm{B}}) - F_k^{(\mathrm{c})}(\theta^{\mathrm{T}})]\delta_{n_x m_x}\delta_{n_y m_y}\end{aligned} \tag{A.6}$$

where the summation over $\tilde{m}$ concerns only the unit cells existing inside the sphere of radius R^{cav} and centred in the i-ion of the $\tilde{n}$ unit cell. It is noteworthy that θ^{B} and θ^{T} as well as $\mathbf{P}$ depend only on the third component of $\tilde{m}$ (i.e. m_z). The primitive function, $F_k^{(\mathrm{c})}$, of the function $f_k^{(\mathrm{c})}$ is given by

$$F_k^{(\mathrm{c})}(\theta) = \begin{cases} F_1^{(\mathrm{c})}(\theta) = -(\sin^2\theta\cos\theta + \frac{2}{3}\cos^3\theta)\\ F_2^{(\mathrm{c})}(\theta) = -(\sin^2\theta\cos\theta + \frac{2}{3}\cos^3\theta)\\ F_3^{(\mathrm{c})}(\theta) = -\frac{2}{3}\cos^3\theta,\end{cases} \tag{A.7}$$

and

$$\theta^{\mathrm{B}} = \arccos\frac{r_3(\tilde{i}_{,1}^{\tilde{n},\tilde{m}})}{R^{\mathrm{cav}}}, \qquad \theta^{\mathrm{T}} = \arccos\frac{r_3(\tilde{i}_{,1}^{\tilde{n},\tilde{m}+\tilde{1}_{\mathrm{c}}})}{R^{\mathrm{cav}}}. \tag{A.8}$$

$(\tilde{m}+\tilde{1}_{\mathrm{c}})$ represents the unit cell having the coordinates (m_x, m_y, m_z+1) located on the top of the $\tilde{m}$ unit cell.

Finally, the Lorentz cavity contribution to the local electric field in the k-direction of the i-ion located in the $\tilde{n}$ unit cell can be rearranged as

$$\begin{aligned}E_k^{\mathrm{cav}}(\tilde{i}^{\tilde{n}}) = \sum_{j=1}^{5}\sum_{\tilde{m}}\frac{\pi}{v(^{\tilde{m}})}\Bigg[&F_k^{(\mathrm{c})}\left(\arccos\frac{r_3(\tilde{i}_{,1}^{\tilde{n},\tilde{m}})}{R^{\mathrm{cav}}}\right)\\ &- F_k^{(\mathrm{c})}\left(\arccos\frac{r_3(\tilde{i}_{,1}^{\tilde{n},\tilde{m}+\tilde{1}_{\mathrm{c}}})}{R^{\mathrm{cav}}}\right)\Bigg]\delta_{n_x m_x}\delta_{n_y m_y} p_k(\tilde{i}_{,j}^{\tilde{n},\tilde{m}}).\end{aligned} \tag{A.9}$$

Note that $\mathbf{r}$, $\mathbf{p}$, and $v(^{\tilde{m}})$ have been defined in subsection 2.2.

Appendix B. The connection between the electronic polarizabilities and the effective electronic polarizabilities

A three-dimensional Taylor series expansion of $p_k^{\mathrm{e}}(\mathbf{E}^{\mathrm{loc}})$ about the point $\mathbf{E}^{\mathrm{loc}} = \mathbf{E}^{\mathrm{spn}}$ ($\mathbf{E}^{\mathrm{spn}}$ is the local electric field in the spontaneous state) defines the α_{kl} element of the first-order electronic polarizability tensor, the $\beta_{kll'}$ element of the second-order electronic polarizability tensor, and the $\gamma_{kll'l''}$ element of the third-order electronic polarizability tensor as follows: [20]

$$p_k^{\mathrm{e}} = p_k^{\mathrm{e}}|_{\mathbf{E}^{\mathrm{loc}}=\mathbf{E}^{\mathrm{spn}}} + \sum_{l=1}^{3}\alpha_{kl}[E_l^{\mathrm{loc}} - E_l^{\mathrm{spn}}] + \tfrac{1}{2}\sum_{l=1}^{3}\sum_{l'=1}^{3}\beta_{kll'}[E_l^{\mathrm{loc}} - E_l^{\mathrm{spn}}][E_{l'}^{\mathrm{loc}} - E_{l'}^{\mathrm{spn}}] + \tfrac{1}{6}\sum_{l=1}^{3}\sum_{l'=1}^{3}\sum_{l''=1}^{3}\gamma_{kll'l''}[E_l^{\mathrm{loc}} - E_l^{\mathrm{spn}}][E_{l'}^{\mathrm{loc}} - E_{l'}^{\mathrm{spn}}][E_{l''}^{\mathrm{loc}} - E_{l''}^{\mathrm{spn}}], \tag{B.1}$$

$$\alpha_{kl} = \left.\frac{\partial p_k^{\mathrm{e}}}{\partial E_l^{\mathrm{loc}}}\right|_{\mathbf{E}^{\mathrm{loc}}=\mathbf{E}^{\mathrm{spn}}}, \tag{B.2}$$

$$\beta_{kll'} = \left.\frac{\partial^2 p_k^{\mathrm{e}}}{\partial E_l^{\mathrm{loc}}\,\partial E_{l'}^{\mathrm{loc}}}\right|_{\mathbf{E}^{\mathrm{loc}}=\mathbf{E}^{\mathrm{spn}}}, \tag{B.3}$$

$$\gamma_{kll'l''} = \left.\frac{\partial^3 p_k^{\mathrm{e}}}{\partial E_l^{\mathrm{loc}}\,\partial E_{l'}^{\mathrm{loc}}\,\partial E_{l''}^{\mathrm{loc}}}\right|_{\mathbf{E}^{\mathrm{loc}}=\mathbf{E}^{\mathrm{spn}}}, \tag{B.4}$$

and

$$p_k^{\mathrm{e}}|_{\mathbf{E}^{\mathrm{loc}}=\mathbf{E}^{\mathrm{spn}}} = \sum_{l=1}^{3}\alpha_{kl}E_l^{\mathrm{spn}} - \tfrac{1}{2}\sum_{l=1}^{3}\sum_{l'=1}^{3}\beta_{kll'}E_l^{\mathrm{spn}}E_{l'}^{\mathrm{spn}} + \tfrac{1}{6}\sum_{l=1}^{3}\sum_{l'=1}^{3}\sum_{l''=1}^{3}\gamma_{kll'l''}E_l^{\mathrm{spn}}E_{l'}^{\mathrm{spn}}E_{l''}^{\mathrm{spn}}. \tag{B.5}$$

The last equation is deduced from equation (B.1) by taking into consideration that $p_k^{\mathrm{e}}|_{\mathbf{E}^{\mathrm{loc}}=0} = 0$.

Equation (B.1) can be rearranged as

$$p_k^{\mathrm{e}} = \sum_{l=1}^{3}\alpha_{kl}^{\mathrm{eff}}E_l^{\mathrm{loc}} + \tfrac{1}{2}\sum_{l=1}^{3}\sum_{l'=1}^{3}\beta_{kll'}^{\mathrm{eff}}E_l^{\mathrm{loc}}E_{l'}^{\mathrm{loc}} + \tfrac{1}{6}\sum_{l=1}^{3}\sum_{l'=1}^{3}\sum_{l''=1}^{3}\gamma_{kll'l''}^{\mathrm{eff}}E_l^{\mathrm{loc}}E_{l'}^{\mathrm{loc}}E_{l''}^{\mathrm{loc}}, \tag{B.6}$$

where

$$\alpha_{kl}^{\mathrm{eff}} = \alpha_{kl} - \sum_{l'=1}^{3}\beta_{kll'}E_{l'}^{\mathrm{spn}} + \tfrac{1}{2}\sum_{l'=1}^{3}\sum_{l''=1}^{3}\gamma_{kll'l''}E_{l'}^{\mathrm{spn}}E_{l''}^{\mathrm{spn}}, \tag{B.7}$$

$$\beta_{kll'}^{\mathrm{eff}} = \beta_{kll'} - \sum_{l''=1}^{3}\gamma_{kll'l''}E_{l''}^{\mathrm{spn}}, \tag{B.8}$$

$$\gamma_{kll'l''}^{\mathrm{eff}} = \gamma_{kll'l''}. \tag{B.9}$$

$\tilde{\alpha}^{\mathrm{eff}}$, $\tilde{\beta}^{\mathrm{eff}}$, and $\tilde{\gamma}^{\mathrm{eff}}$ are, respectively, the first-, second-, and third-order *effective* electronic polarizability tensors.

References

[1] Watanabe Y, Matsumoto Y, Kunitomo H, Tanamura M and Nishimoto E 1994 *Japan. J. Appl. Phys.* **33** 5182
[2] Funakubo H, Nagano D, Saiki A, Inagaki Y, Shinozaki K and Mizutani N 1997 *Japan. J. Appl. Phys.* **34** 5879
[3] Xuan L, Pan S, Chen Z, Wang R, Shi W and Li C 1998 *Appl. Phys. Lett.* **73** 2896
[4] Yoneda Y, Okabe T, Sakaue K and Terauchi H 1998 *J. Appl. Phys.* **83** 2458
[5] Zhao T, Chen F, Lu H, Yang G and Chen Z 2000 *J. Appl. Phys.* **87** 7442
[6] Zhao T, Lu H, Chen F, Yang G and Chen Z 2000 *J. Appl. Phys.* **87** 7448

[7] Yoneda Y, Sakaue K and Terauchi H 2001 *J. Phys.: Condens. Matter* **13** 9575
[8] Petraru A, Schubert J, Schmid M and Buchal Ch 2002 *Appl. Phys. Lett.* **81** 1375
[9] Junquera J and Ghosez P 2003 *Nature* **422** 506
[10] El Marssi M, Le Marrec F, Lukyanchuk I A and Karkut M G 2003 *J. Appl. Phys.* **94** 3307
[11] Schubert J, Trithaveesak O, Petraru A, Jia C L, Uecker R, Reiche P and Schlom D G 2003 *Appl. Phys. Lett.* **82** 3460
[12] Tabata H, Tanaka H, Kawai T and Okuyama M 1995 *Japan. J. Appl. Phys.* **34** 544
[13] Zhao T, Chen Z, Chen F, Shi W, Lu H and Yang G 1999 *Phys. Rev.* B **60** 1697
[14] Shimuta T, Nakagawara O, Makino T, Arai S, Tabata H and Kawai S 2002 *J. Appl. Phys.* **91** 2290
[15] Jiang A Q, Scott J F, Lu H and Chen Z 2003 *J. Appl. Phys.* **93** 1180
[16] Ríos S, Ruediger A, Jiang A Q, Scott J F, Lu H and Chen Z 2003 *J. Phys.: Condens. Matter* **15** L305
[17] Kay H E and Vousden P 1949 *Phil. Mag.* **7** 1019
[18] Chaib H, Khatib D and Kinase W 1999 *Nonlinear Opt.* **23** 97
[19] Chaib H, Otto T and Eng L M 2003 *Phys. Rev.* B **67** 174109
[20] Sauer S P A 1997 *J. Phys. B: At. Mol. Opt. Phys.* **30** 3773
[21] Slater J C 1930 *Phys. Rev.* **34** 57
[22] Slater J C 1950 *Phys. Rev.* **78** 748
[23] Lawless W N 1965 *Phys. Rev.* **138** A1751
Forsbergh P W 1949 *Phys. Rev.* **76** 1187
[24] Levin S B, Field N J, Plock F W and Merker L 1955 *J. Opt. Soc. Am.* **45** 737
[25] Kittel C 1996 *Introduction to Solid State Physics* (New York: Wiley)
[26] Yariv A and Yeh P 1984 *Optical Waves in Crystals* (New York: Wiley–Interscience)
Sirotine Y and Chaskolskaia M 1984 *Fondements de la Physique des Cristaux* (Moscow: Mir)
[27] Heifets E, Eglitis R I, Kotomin E A, Maier J and Borstel G 2001 *Phys. Rev.* B **64** 235417
[28] Jona F and Shirane J 1962 *Ferroelectric Crystals* (Oxford: Pergamon)
[29] Toumanari A 1999 *PhD Thesis* University of Agadir, Morocco
[30] Nakamura K and Kinase W 1992 *J. Phys. Soc. Japan* **61** 2114
[31] Nakamura K and Kinase W 1992 *J. Phys. Soc. Japan* **61** 4596
[32] Cudney R S, Fousek J, Zgonik M and Günter P 1993 *Appl. Phys. Lett.* **63** 3399
[33] Baudry L and Tournier J 2001 *J. Appl. Phys.* **90** 1442
[34] Shih W Y, Shih W H and Aksay I A 1994 *Phys. Rev.* B **50** 15575
[35] Ishikawa K and Uemori T 1999 *Phys. Rev.* B **60** 11841
[36] Lu T and Cao W 2002 *Phys. Rev.* B **66** 024102
[37] Tinte S and Stachiotti M G 2001 *Phys. Rev.* B **64** 235403